Role of Triplet–Triplet Annihilation in Anthracene Dimerization[1a]

James L. Charlton,*[1b] Reza Dabestani,[1c] and Jack Saltiel*[1c]

Contribution from the Departments of Chemistry, The Florida State University, Tallahassee, Florida 32306, and The University of Manitoba, Winnipeg, Manitoba, Canada R3T 2N2.
Received November 19, 1982

Abstract: The dependence of anthracene dimerization quantum yields on light intensity in degassed, but not in air-saturated, solutions establishes a significant triplet–triplet annihilation component leading to dimer. An excellent fit of observed quantum yields over wide concentration and intensity ranges to derived expressions is obtained by employing computer assistance and mainly literature rate constants. The single derived parameter is $p_e' = 0.115 \pm 0.007$, the fraction of triplet–triplet encounter pairs that give the precursor to dimer. This value suggests a strict adherence to the spin-statistical factor of 1/9 for formation of the singlet component of the annihilation event and confirms a previous conclusion that higher spin states of the encounter pair, being dissociative, do not provide a pathway to dimer. The relationship of these observations to the theory of photocycloaddition reactions is considered.

Introduction

Allowed concerted photocycloadditions are usually postulated to involve singlet excimer or exciplex intermediates,[2] as demonstrated compellingly in some instances by using exciplex specific quenchers.[3,4] Theoretical treatments suggest that the path to adduct requires passing from the singly excited complex into a doubly excited electronic state which correlates with the ground states of addends and adducts.[2,5] Avoided crossing between appropriate correlation lines creates a pericyclic minimum on the doubly excited surface. Decay through a "funnel" or "hole" at this minimum allows for return to ground-state addends and formation of adduct(s). On the addend side the doubly excited state can be thought as arising through interaction of the lowest triplet states of each addend.[2,5]

In practice, the interaction of two triplets of the same molecule in solution provides an important triplet decay channel known as triplet–triplet annihilation, TTA. Though it often gives rise to monomer and excimer delayed fluorescence,[6,7] its role in photochemical reactions had not been examined. Anthracene, (A) photodimerization, one of the oldest known photochemical reactions,[8] is believed to occur via a singlet excimer, $^1(AA)^*$, intermediate.[9] The theoretical discription given above is applied to this reaction in Figure 1. TTA-induced photodimerization was first proposed[10] to account for dianthracene (A_2) formation following triplet excitation transfer from biacetyl to anthracene.[11] This pathway was also proposed in accounting for the spin-statistical factor in TTA of anthracene triplets.[12] In this paper are reported observations concerning the dependence of A_2 quantum yields, ϕ_{A_2}, for direct A excitation on light intensity, I_a, which allow a quantitative evaluation of the TTA component in photodimerization.

Scheme I

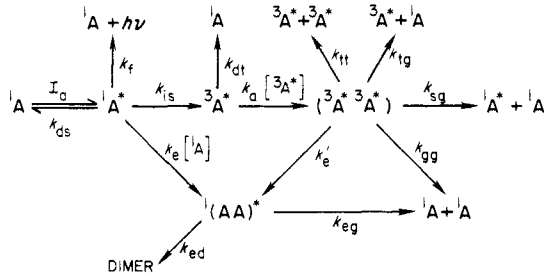

Results

Solutions of anthracene in benzene were degassed using six freeze–pump–thaw cycles to less than 10^{-5} torr and flame sealed. The samples were irradiated in Pyrex ampules in a merry-go-round apparatus[13] immersed in a thermostated water bath, 30 °C, using the 366-nm line of 200-, 450- and 550-W Hanovia mercury lamps. Incident light intensities were measured using benzophenone-sensitized trans–cis isomerization of stilbene as the actinometer, $\phi_{t\to c} = 0.55$.[14] Photodimerization quantum yields at various light intensities and anthracene concentrations are given in Table I. A set of quantum yields obtained in the presence of air is also included.

Discussion

Scheme I, which has been used to represent the photophysical processes for anthracene,[12] was employed. ($^3A^*{}^3A^*$) represents the two triplet encounter pair, and the remaining terms are self-explanatory. The sum of the limiting dimerization quantum yield from the singlet excimer[9b] and the photocleavage quantum yield of A_2[15] is nearly unity, suggesting efficient formation of a common intermediate from which decay to 2A and A_2 occurs. This intermediate probably corresponds to the pericyclic minimum on the double excited surface, Figure 1. Since conversion of the

(1) (a) Work at Florida State University supported by National Science Foundation Grant Nos. CHE 80-26701 and CHE 77-23582. (b) University of Manitoba. (c) Florida State University.
(2) Caldwell, R. A. *J. Am. Chem. Soc.* **1980**, *102*, 4004.
(3) (a) Caldwell, R. A.; Creed, D. *Acc. Chem. Res.* **1980**, *13*, 45. (b) Caldwell, R. A.; Smith, L. *J. Am. Chem. Soc.* **1974**, *96*, 2994. (c) Caldwell, R. A.; Creed, D.; DeMarco, D. C.; Melton, L. A.; Ohta, H.; Wine, P. H. *Ibid.* **1980**, *102*, 2369.
(4) (a) Majima, T.; Pac, C.; Sakurai, H. *Bull. Chem. Soc. Jpn.* **1978**, *51*, 1811. (b) Pac, C.; Sakurai, H. *Chem. Lett.* **1976**, 1067. (c) Itoh, M.; Takita, N.; Matsumoto, M. *J. Am. Chem. Soc.*, **1979**, *101*, 7363.
(5) See especially: (a) Michl, J. *Pure Appl. Chem.* **1975**, *41*, 507. (b) Michl, J. *Photochem. Photobiol.* **1977**, *25*, 141, and references cited.
(6) Stevens, B.; Hutton, E. *Nature (London)* **1960**, *186*, 1045.
(7) (a) Parker, C. A.; Hatchard, C. G. *Proc. Chem. Soc.* **1962**, 147. (b) Parker, C. A.; Hatchard, C. G. *Trans. Faraday Soc.* **1963**, *59*, 284. (c) Parker, C. A. *Adv. Photochem.* **1964**, *2*, 305.
(8) Fritzsche, J. *J. Pract. Chem.* **1867**, *101*, 337; **1869**, *106*, 274.
(9) For reviews see (a) Stevens, B. *Adv. Photochem.* **1971**, *8*, 171. (b) Saltiel, J.; Townsend, D. E.; Watson, B. D.; Shannon, P.; and Finson, S. L. *J. Am. Chem. Soc.* **1977**, *99*, 884.
(10) Saltiel, J. *Surv. Prog. Chem.* **1964**, *2*, 239.
(11) Bäckstrom, H. L. J.; Sandros, K. *Acta Chem. Scand.* **1958**, *12*, 823.
(12) Saltiel, J.; Marchand, G. R.; Smothers, W. K.; Stout, S. A.; Charlton, J. L. *J. Am. Chem. Soc.* **1981**, *103*, 7159.
(13) Moses, F. G.; Liu, R. S. H.; Monroe, B. M. *Mol. Photochem.* **1969**, *1*, 245.
(14) (a) Hammond, H. A.; DeMeyer, D. E.; Williams, J. L. R. *J. Am. Chem. Soc.* **1969**, *91*, 5180. (b) Valentine, D., Jr.; Hammond, G. S. *Ibid.* **1972**, *94*, 3449.
(15) Wei, K. S.; Livingston, R. *Photochem. Photobiol.* **1967**, *6*, 229.

0002-7863/83/1505-3473$01.50/0

Table I. Dimer Quantum Yields[a]

$10^3\phi_{A_2}$ obsd	$10^3\phi_{A_2}$ calcd	$10^3[\bar{A}]$,[b] M	$10^9 I_a$, einstein s^{-1}	$10^3\phi_{A_2}$ obsd	$10^3\phi_{A_2}$ calcd	$10^3[\bar{A}]$,[b] M	$10^9 I_a$, einstein s^{-1}
			Set 1				
4.1_9	3.84	0.29_2	0.37_8	$11._6$	11.1	0.72_8	3.6_2
8.2_0	11.2	0.29_0	4.7_6	$12._2$	12.6	1.4_5	0.37_4
8.1_0	9.97	0.28_9	3.6_5	$16._1$	15.9	1.4_5	4.6_6
5.7_0	4.83	0.44_0	0.37_8	$16._6$	15.6	1.5_0	3.6_2
9.6_0	11.1	0.44_2	4.7_6	$26._5$	28.5	3.6_7	0.37_4
9.9_8	10.0	0.43_9	3.6_5	$26._6$	30.1	3.7_0	4.4_6
5.8_3	5.88	0.58_3	0.37_7	$26._7$	29.1	3.5_6	3.6_4
$10._7$	11.4	0.58_3	4.6_7	$45._0$	50.9	7.4_5	0.37_4
$10._1$	10.4	0.57_7	3.6_2	$45._9$	51.7	7.4_8	4.4_6
7.6_8	6.96	0.72_5	0.37_7	$42._7$	50.8	7.3_4	3.6_4
$12._0$	12.0	0.73_6	4.6_7				
			Set 2				
6.3_5	6.64	0.28_3	1.5_2	$13._3$	10.7	0.73_6	3.1_8
$10._0$	11.4	0.23_5	4.7_3	$14._8$	14.0	1.5_0	1.5_2
9.8_8	9.38	0.27_8	3.1_8	$17._6$	15.8	1.4_3	4.7_3
7.1_4	7.13	0.43_6	1.5_2	$18._9$	15.3	1.5_1	3.1_8
$10._4$	11.0	0.38_1	4.7_3	$25._1$	30.1	3.8_4	1.5_2
$10._8$	9.46	0.43_0	3.1_8	$29._6$	30.3	3.7_1	4.7_3
8.1_3	7.91	0.58_8	1.5_2	$30._2$	30.8	3.8_6	3.1_8
$11._4$	11.3	0.52_9	4.7_3	$40._2$	52.5	7.7_4	1.5_2
$12._0$	9.97	0.58_3	3.1_8	$44._6$	52.1	7.5_6	4.7_3
5.6_5[c]	8.97	0.76_4	1.5_2	$33._5$	53.3	7.8_4	3.1_8
$12._1$	11.8	0.68_0	4.7_3				
			Set 3[d]				
3.2_9	2.13	0.28_8	4.8_5	4.7_7	5.30	0.72_8	4.8_5
1.9_7	2.23	0.30_2	3.2_7	$10._8$	10.4	1.4_6	4.8_5
2.1_0	2.25	0.30_5	4.8_5	$11._0$	10.4	1.4_6	4.8_5
3.1_6	3.26	0.44_4	4.8_5	$16._0$	24.7	3.7_3	4.8_5
3.6_6	3.26	0.44_4	4.8_5	$21._8$	24.3	3.6_7	4.8_5
5.6_6	4.25	0.58_2	4.8_5	$42._0$	43.6	7.3_0	4.8_5
3.2_2	4.23	0.57_8	3.2_7	$41._0$	44.5	7.4_9	4.8_5
5.1_6	5.35	0.73_5	4.8_5				

[a] Corning CS 7-37 and CS 0-52 filters were employed. [b] Average anthracene concentrations; range of initial concentrations for sets 1 and 3 was $(0.32_1\text{–}8.0_4) \times 10^{-3}$ M and for set 2 $(0.32_0\text{–}8.0_0) \times 10^{-3}$ M. [c] Air contamination suspected; see Figure 1. [d] Air-saturated solutions.

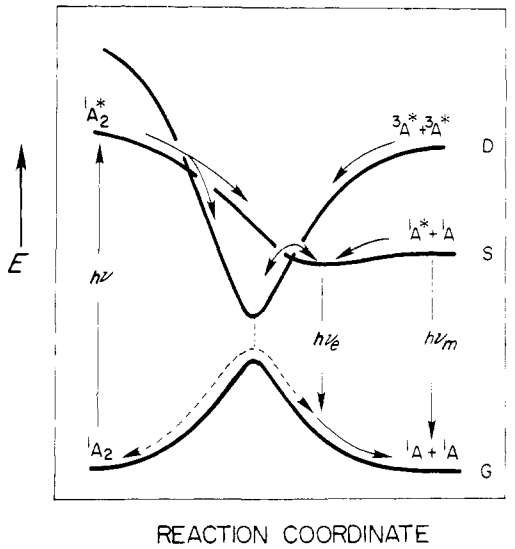

Figure 1. Potential energy diagrams showing the two paths to anthracene photodimerization.[5]

singly excited to the doubly excited singlet excimer appears to be the only significant fate of the former, no distinction between these two intermediates is made in Scheme I.

The steady-state solution for the dimer quantum yield is

$$\phi_{A_2} = \frac{p_{ed}}{I_a}\left[\frac{I_a k_e[^1A]}{C} + \left(\frac{p_s k_e[^1A]}{C} + p_e'\right) k_a[^3A^*]_{ss}^2\right] \quad (1)$$

where $p_{ed} = k_{ed}/(k_{ed} + k_{eg})$, $p_s = k_{sg}/G$, $p_e' = k_e'/G$, $C = (k_{ds} + k_{is} + k_f + k_e[^1A])$, $G = (k_{tt} + k_{tg} + k_{sg} + k_{gg} + k_e')$, and $[^3A^*]_{ss}$, the steady-state triplet concentration, is given by

$$[^3A^*]_{ss} = \frac{k_{dt} - \left[k_{dt}^2 - 4k_a\left(-2 + p_t + \frac{p_s k_{is}}{C}\right)\frac{k_{is} I_a}{C}\right]^{1/2}}{2k_a\left(-2 + p_t + \frac{p_s k_{is}}{C}\right)} \quad (2)$$

where $p_t = (2k_{tt} + k_{tg})/G$; see Appendix. The quenching of $^3A^*$ by ground-state anthracene

$$^3A^* + {}^1A \xrightarrow{k_{sq}} 2\,{}^1A \quad (3)$$

though not included in Scheme I, has been demonstrated unequivocally in this laboratory.[16] Accordingly, the rate constant for $^3A^*$ decay, k_{dt}, is given by $k_{dt} = k_{dt}^0 + k_{sq}[^1A]$.[16] Since some of the quantum yields were measured in the presence of air, the above equations must also be modified to include oxygen quenching of the excited species;[9b,17] i.e., the known terms $k_{qs}[O_2]$ and $k_{qt}[O_2]$ were included in k_{dt} and C, respectively.

For the calculations, it was assumed that the path length was 1.33 cm and that light intensity was uniform over the entire irradiated area (1.34 cm^2). Light is absorbed nonuniformly by the sample, decreasing exponentially with depth over the exposed portion of the solution (only ~1.7 mL of the 6.0-mL sample is in the light path). Absorbed light and yield of dimer were cal-

(16) Saltiel, J.; Marchand, G. R.; Dabestani, R., manuscript in preparation.

(17) (a) Stevens, B.; Algar, B. E. *Ann. N.Y. Acad. Sci.* **1970**, *171*, 50. (b) Patterson, L. K.; Porter, G.; Topp, M. R. *Chem. Phys. Lett.* **1970**, *7*, 612. (c) Gijzeman, O. L. J.; Kaufman, K.; Porter, G. *J. Chem. Soc., Faraday Trans. 2* **1973**, *69*, 708.

Table II. Parameters Used in Computing Dimer Quantum Yields

parameter	value	ref
p_t	1.40	12
p_s	0.046	12
p_{ed}	0.22	9b
k_a	9.6×10^9 M^{-1} s^{-1}	9b, 18
k_e	9.6×10^9 M^{-1} s^{-1}	9b[a,b]
k_f	6.43×10^7 s^{-1}	19[a,c]
k_{is}	1.74×10^8 s^{-1}	20[a,d]
k_{ds}	0	20[d]
$k_{qs}[O_2]$	4.5×10^7 M^{-1} s^{-1}	9b[e]
$k_{qt}[O_2]$	5.6×10^6 M^{-1} s^{-1}	12[c]
k_{dt}^0	49 s^{-1}	16
k_{sq}	3.73×10^5 M^{-1} s^{-1}	16
p_e	0.115 ± 0.007	(calcd)

[a] Based on 4.2 ns, the lifetime of ^{1}A* in benzene; see ref 36 in ref 9b. [b] The value of $k_e\tau_m$ from ref 9b adjusted for the change in T/η. [c] The average $\phi_f = 0.27$ was used. [d] $\phi_{is} + \phi_f = 1.00$ was assumed; ref 20 gives $\phi_{is} = 0.72$. [e] The value for 25 °C was used.[9b]

culated for small increments of the solution and these then summed over the entire solution to obtain the average quantum yields; see Appendix. Because of the complexity of the equations and the necessity for numerical integration, computer assistance was employed to calculate the dimer quantum yield as a function of $[^1\bar{A}]$ and I_a. Good literature values are available for all parameters in eq 1 and 2 except p_e' (Table II). An iterative fitting routine was therefore used to adjust p_e' while minimizing the difference between computed and observed yields. Calculated quantum yields are listed in Table I, and values for selected runs are plotted in Figure 2. Despite the high intensity, a linear relationship between $1/\phi_{A_2}$ and $1/[^1\bar{A}]$ is observed for air-saturated solutions since oxygen quenching of ^{3}A* eliminates the TTA contribution to dimer formation.[21] For the degassed solutions the curvature of the plots, being more pronounced at higher intensities, reflects the contribution of TTA to dimer formation. At the higher anthracene concentrations the calculated lines in Figure 1 converge because self-quenching, eq 3, reduces the lifetime of ^{3}A* and diminishes the role of TTA as a decay process. The failure of previous quantitative studies to reveal the TTA anthracene dimerization component can thus be traced to the use of high anthracene concentrations.[9b,22] The self-quenching process and not the low light intensities employed ($\sim 1 \times 10^{-9}$ einstein s^{-1})[22c] accounts for the reported insensitivity of ϕ_{A_2} on I_a.

The best fit value for p_e', the fraction of TT encounter pairs that give the singlet excimer precursor to dimer ($p_e' = 0.115 \pm 0.007$), is indistinguishable from 1/9, the spin-statistical factor for the formation of the singlet component of TTA. It thus appears that of the nine spin states formed, only the singlet has an efficient pathway to dimer. This result is gratifying because it is consistent with the mechanism proposed to account for the deviation of the effective TTA rate constant from the rate constant for a diffusion-controlled reaction.[12]

TTA has been established to play a significant role in anthracene photodimerization under conditions ordinarily employed to measure quantum yields. It may be important in many other photochemical reactions, particularly those carried out at high light intensities. Sensitized dimerization of anthracene should proceed exclusively by the TTA route.[10,11] Initial results with

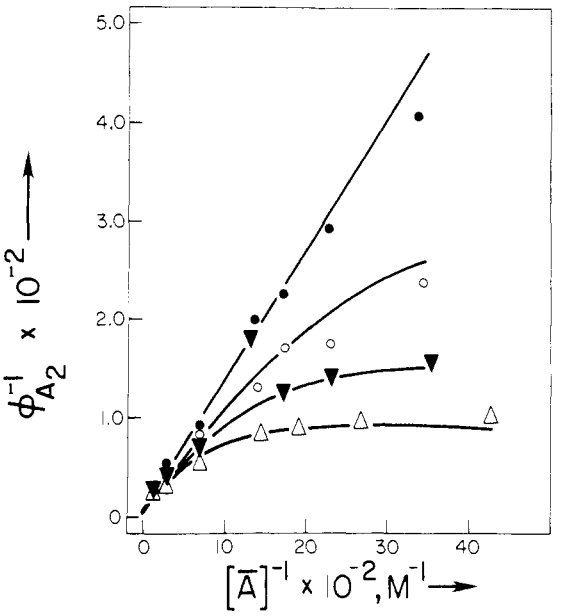

Figure 2. The dependence of dimer quantum yields on intensity and anthracene concentration; points are from representative runs and lines are through calculated values: (△) set 2, $I_a = 4.73 \times 10^{-9}$ einstein s^{-1}; (▼) set 2, $I_a = 1.52 \times 10^{-9}$ einstein s^{-1}; (○) set 1, $I_a = 0.38 \times 10^{-9}$ einstein s^{-1}; (●) set 3, air, points are averages of observed values.

fluorenone as the sensitizer follow a general trend consistent with the parameters in Table II. Anticipated future experiments in this area should determine whether ^{13}C enhances anthracene photodimerization via TTA by introducing intersystem crossing steps between quintet and/or triplet and singlet TT encounter pairs.[23] It is important to note that the results in this paper provide the first experimental evidence showing that the postulated doubly excited singlet state[5] is indeed a viable intermediate for photocycloaddition.

Experimental Section

Materials. Benzene (Mallinkrodt reagent grade) was purified by the Metts exhaustive photochlorination procedure[12] and stored over sodium. Anthracene, synthesized[24] from benzene and phthalic anhydride (Mallinkrodt analytical reagent), was recrystallized, chromatographed on alumina, and sublimed twice, mp 216.5–217.5 °C. Materials used for stilbene actinometry have been previously described.[25]

Quantum Yields. Solutions (6.00 mL each) were syringed into Pyrex ampules (inside diameter 1.33 cm) equipped with 14/35 female joints and grease traps. The solutions were degassed using six freeze–pump–thaw cycles and flame sealed at a constriction. Air-saturated solutions were employed in two runs. Irradiations were performed in a Moses merry-go-round apparatus[12] immersed in a thermostated water bath, 30 °C, using 200-, 450-, and 550-W Hanovia medium-pressure mercury lamps. Corning CS 7-37 and 0-52 filters were used to isolate the 366-nm mercury lines. In one run double sets of these filters were employed in order to obtain a lower light intensity. The samples were irradiated through rectangular windows, 0.71 cm × 1.88 cm, so that only 1.69 mL of the solutions was in the light path. Anthracene loss was determined by UV analysis (Cary 14, 379.0 nm) of diluted solutions; zero-time solutions were employed as reference. Anthracene concentrations reported in Table I are averages of initial and final concentrations; initial concentrations were $[A]_0 \times 10^3$, M: 0.32, 0.48, 0.64, 0.80, 1.6, 4.0, and 8.0 (see also footnote *c*, Table I). Conversions to *cis*-stilbene in actinometer solutions were determined by GLC and corrected for back reaction and initial cis content as previously described.[25] For the lowest anthracene concentration a small correction was applied to the quantum yield to account for incomplete light absorption. More details on the treatment of the data are given in the Appendix.

(18) Saltiel, J.; Shannon, P. T.; Zafiriou, O. C.; Uriarte, A. K. *J. Am. Chem. Soc.* **1980**, *102*, 6799.
(19) (a) Dawson, W. R.; Windsor, M. W. *J. Phys. Chem.* **1968**, *72*, 3251. (b) Birks, J. B.; Dyson, D. J. *Proc. R. Soc. London, Ser. A* **1963**, *275*, 135. (c) Weber, G.; Teale, F. W. J. *Trans. Faraday Soc.* **1957**, *53*, 646. (d) Melhuish, W. H. *J. Phys. Chem.* **1961**, *65*, 229.
(20) Horrocks, A. R.; Wilkinson, F. *Proc. R. Soc. London, Ser. A* **1968**, *306*, 257.
(21) This applies also to results reported in: Bowen, E. J.; Tanner, D. W. *Trans. Faraday Soc.* **1955**, *51*, 475.
(22) (a) Cowan, D. W.; Schmiegel, W. W. *J. Am. Chem. Soc.* **1972**, *94*, 6779. (b) Vember, T.; Veselova, T. V.; Obyknovennaya, I. E.; Cherkasov, A.; Shirokov, V. *Izv. Akad. Nawk SSSR, Ser. Fiz.* **1973**, *37*, 837. (c) Castellan, A.; Lapouyade, R.; Bouas-Laurent, H. *Bull. Soc. Chim. Fr.* **1976**, 201. (d) Yang, N. C.; Shold, D. M.; Kim, B. *J. Am. Chem. Soc.* **1976**, *98*, 6587.
(23) Excellent analogy is provided by the effect of ^{13}C on radical–radical coupling reactions: (a) Turro, N. J.; Chow, M.-F.; Chung, C.-J.; Krauetler, B. *J. Am. Chem. Soc.* **1981**, *103*, 3886. (b) Turro, N. J.; Anderson, D. R.; Chow, M.-F.; Chung, C.-J.; Krauetler, B. *Ibid.* **1981**, *103*, 3892.
(24) Fieser, L. F.; Williamson, K. L. "Organic Experiments", 4th ed.; Heath: Lexington, Mass., **1979**; p 260.
(25) Saltiel, J.; Marinari, A.; Chang, D. W.-L.; Mitchener, J. C.; Megarity, E. D. *J. Am. Chem. Soc.* **1979**, *101*, 2982.

Appendix

Derivation of Eq 1 and 2. Five differential equations follow directly from Scheme I:

$$d[^1A^*]/dt = I_a + k_{sg}[(^3A^*{}^3A^*)] - (k_f + k_e[^1A] + k_{is})[^1A^*] \quad (4)$$

$$d[^3A^*]/dt = k_{is}[^1A^*] + (2k_{tt} + k_{tg})[(^3A^*{}^3A^*)] - (k_{dl} + 2k_a[^3A^*])[^3A^*] \quad (5)$$

$$d[(^3A^*{}^3A^*)]/dt = k_a[^3A^*]^2 - (k_{tt} + k_{tg} + k_{sg} + k_e' + k_{gg})[(^3A^*{}^3A^*)] \quad (6)$$

$$d[^1(AA)^*]/dt = k_e[^1A^*][^1A] + k_e'[(^3A^*{}^3A^*)] - (k_{ed} + k_{eg})[^1(AA)^*] \quad (7)$$

$$d[A_2]/dt = k_{ed}[^1(AA)^*] \quad (8)$$

We proceed by applying the steady-state approximation to all excited species. From eq 6

$$[(^3A^*{}^3A^*)]_{ss} = k_a[^3A^*]_{ss}^2/G \quad (9)$$

where $G = (k_{tt} + k_{tg} + k_{sg} + k_e' + k_{gg})$ is the sum of the rate constants for all processes which destroy triplet encounter pairs. From eq 4

$$[^1A^*]_{ss} = (I_a + p_s k_a[^3A^*]_{ss}^2)/C \quad (10)$$

where $p_s = k_{sg}/G$ is the fraction of $(^3A^*{}^3A^*)$ which give monomer $^1A^*$ directly, and $C = (k_f + k_{is} + k_e[^1A])$ is the overall decay rate of $^1A^*$. From eq 7

$$[^1(AA)^*]_{ss} = (k_e[^1A][^1A^*]_{ss} + k_e'[(^3A^*{}^3A^*)_{ss}])/(k_{ed} + k_{eg}) \quad (11)$$

which can be combined with eq 9 and 10 to give

$$[^1(AA)^*]_{ss} = \{I_a k_e[^1A] + (p_s k_e[^1A] + Cp_e')k_a[^3A^*]^2\}/C(k_{ed} + k_{eg}) \quad (12)$$

Combining eq 5 with eq 9 and 10 gives

$$d[^3A^*]/dt = k_{is}(I_a + p_s k_a[^3A^*]_{ss}^2)/C + (2k_{tt} + k_{tg})(k_a[^3A^*]_{ss}^2/G) - k_{dt}[^3A^*]_{ss} - 2k_a[^3A^*]_{ss}^2 \quad (13)$$

which together with the steady-state approximation for $[^3A^*]$ can be rearranged to give

$$k_a[^3A^*]_{ss}^2[-2 + p_t + p_s k_{is}/C] - k_{dt}[^3A^*]_{ss} + k_{is}I_a/C = 0 \quad (14)$$

where $p_t = (2k_{tt} + k_{tg})/G$ is the average number of triplets produced by dissociation or decay of a given TT encounter pair. Using the quadratic formula, eq 2 is readily obtained from eq 14. The quantum yield for dimer formation, eq 1, can be obtained by substituting the expression for $[^1(AA)^*]_{ss}$, eq 12, into

$$\phi_{A_2} = k_{ed}[^1(AA)^*]_{ss}/I_a \quad (15)$$

and defining $p_{ed} = k_{ed}/(k_{ed} + k_{eg})$, the fraction of singlet excimers which give dimer. As indicated in the Discussion section self-quenching and oxygen quenching can be included in eq 1 and 2 by replacing every occurrence of k_{dt} by $k_{dt}^0 + k_{sq}[^1A] + k_{qt}[O_2]$ and expanding C by adding the term $k_{qs}[O_2]$.

Nonuniform Absorption and Bimolecular Excited State Reactions. Owing to the nature of light absorption, the concentration of excited states decreases logarithmically away from the irradiated surface of a solution. This nonuniform concentration presents a problem in calculating quantum yields of processes involving bimolecular reactions of excited states because such yields are not linearly dependent on excited-state concentrations. Experimentally, the problem is often avoided by using solutions of low absorbance in which excited-state production can be assumed uniform throughout. Since this is not always desirable or practical and does not apply to the conditions employed in this work, the following method was employed in computing average quantum yields for solutions of high absorbance.

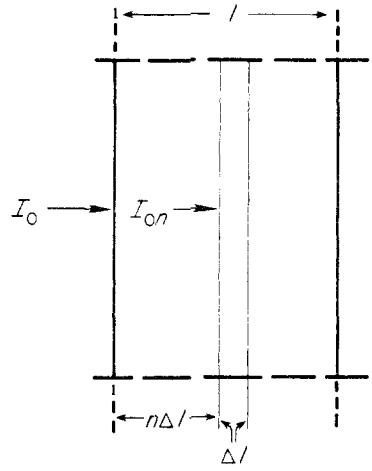

Figure 3. Cross section showing irradiated portion of ampule.

The approach used involves dividing the solution into m segments of depth Δl cm and calculating excited-state concentrations and quantum yields for each incremental segment (Figure 3). The average quantum yield is then calculated by averaging over all m segments. The light absorbed within the nth incremental segment, I_{an}, of depth Δl is given by

$$I_{an} = I_{on}(1 - 10^{-\epsilon c \Delta l}) \quad (16)$$

where c is the concentration of the absorbing molecule, and I_{0n}, the light intensity impingent on the nth segment, is given by

$$I_{0n} = I_0 10^{-\epsilon c n \Delta l} \quad (17)$$

where I_0 is the incident intensity at the front surface of the solution and $n\Delta l$ is the distance of the nth segment from the front surface. Combining eq 16 and 17 gives

$$I_{an} = I_0 10^{-\epsilon c n \Delta l}(1 - 10^{-\epsilon c \Delta l}) \quad (18)$$

Since Δl is in cm and I_0 is expressed in einstein s^{-1} cm^{-2}, I_{an} is converted to einstein s^{-1} L^{-1} by dividing by $\Delta l \times 10^{-3}$. The product yield within the nth segment, Y_n, can now be calculated from the functional relationship between yield and absorbed light; see preceding section. Since Y_n is expressed in M s^{-1}, converting to mol s^{-1} requires multiplication by $A\Delta l$ where A is the irradiated area. The total product yield, Y, is obtained by summing over all m increments,

$$Y = A\Delta l \sum_{n=0}^{m} Y_n \quad (19)$$

Since the total light absorbed in einstein s^{-1}, I_a, is given by

$$I_a = I_0(1 - 10^{-\epsilon c l})A \quad (20)$$

where $l = m\Delta l$, the average quantum yield, ϕ_{av}, is calculated from

$$\phi_{av} = \Delta l \sum_{n=0}^{m} Y_n / I_0(1 - 10^{-\epsilon c l}) \quad (21)$$

Samples were divided into 100 segments and ϕ_{av} values calculated using computer assistance. It was shown that there is practically no change in p_e' and calculated quantum yields on increasing n from 100 to 1000. However, if integration of yields over the depth of the cell is not applied ($n = 1$), then the standard deviation in Y increases from 16 to 20% and an effective value of $p_e' = 0.178 \pm 0.015$ is obtained.

Registry No. Anthracene, 120-12-7.